Sensors and Actuators B 203 (2014) 719–725

Contents lists available at ScienceDirect

Sensors and Actuators B: Chemical

journal homepage: www.elsevier.com/locate/snb

A sensitive and selective fluorescent sensor for Zinc(II) and its application to living cell imaging

Hao-Ming Liu, Parthiban Venkatesan, Shu-Pao Wu*

Department of Applied Chemistry, National Chiao Tung University, Hsinchu 300, Taiwan, Republic of China

ARTICLE INFO

Article history:
Received 29 May 2014
Received in revised form 10 July 2014
Accepted 12 July 2014
Available online 21 July 2014

Keywords:
Sensors
Zn(II)
Fluorescence
Imaging agents

ABSTRACT

A new dipyrromethene derivative (**DP1**) exhibits an enhanced fluorescence in the presence of Zn^{2+} ions and a high selectivity for Zn^{2+} ions over competing metal ions in methanol; Ag^{+}, Ca^{2+}, Co^{2+}, Cr^{3+}, Fe^{2+}, Fe^{3+}, Hg^{2+}, K^{+}, Mg^{2+}, Mn^{2+}, Ni^{2+}, and Pb^{2+} produced only minor changes in the fluorescence of **DP1**. The binding ratio of the **DP1**–Zn^{2+} complexes was determined from a Job plot to be 1:1. The binding constant (K_a) of Zn^{2+} binding to **DP1** was found to be $6.12 \times 10^4\ M^{-1}$, with a detection limit of 0.236 μM. Fluorescence microscopy imaging using RAW264.7 cells showed that **DP1** could be used as an effective fluorescent probe for detecting Zn^{2+} in living cells.

1. Introduction

The development of fluorescent chemosensors for detecting biologically important metal ions, such as Fe^{3+}, Cu^{2+}, and Zn^{2+}, has been an important research topic. Among the transition metal ions, zinc is the second most abundant in the human body, after iron. Zinc ions are mostly bound within proteins and play various key roles in biological systems, including neural signal transmission [1], enzyme regulation [2], apoptosis [3], and gene transcription [4]. Disorders in Zn^{2+} metabolism have been linked to several severe neurological diseases, including Alzheimer's disease (AD) [5,6], cerebral ischemia [7], and epilepsy [8]. Therefore, the measurement of Zn^{2+} is important in monitoring biological processes.

Several methods for Zn^{2+} detection in various samples have been developed, such as atomic absorption-emission spectroscopy [9], inductively coupled plasma-atomic emission spectrometry (ICP-AES) [10,11], and voltammetry [12]. Although these methods provide quantitative data, most of them require expensive instruments, and are not appropriate for direct analysis. Recently, more attention has been focused on the development of fluorescent probes for detecting Zn^{2+} ions in biological and environmental samples [13–28].

In this study, a fluorescent chemosensor **DP1** has been designed for metal ion detection. **DP1** consists of a dippyromethene and a benzoimidazole moiety (Scheme 1). The metal ions Ag^{+}, Ca^{2+}, Cd^{2+}, Co^{2+}, Cu^{2+}, Fe^{2+},Fe^{3+}, Hg^{2+}, Mg^{2+}, Mn^{2+}, Ni^{2+}, and Pb^{2+} were tested with chemosensor **DP1**; Zn^{2+} was the only ion that caused strong fluorescent enhancement upon binding with chemosensor **DP1**, producing a "turn-on" type chelation-enhanced fluorescence (CHEF) sensor.

2. Materials and methods

2.1. Materials and instrumentation

All reagents were obtained from commercial sources and used as received without further purification. UV–vis spectra were recorded on an Agilent 8453 UV–vis spectrometer. Fluorescence spectra were recorded in a Hitachi F-4500 spectrometer. ^1H and ^{13}C NMR spectra were recorded on Bruker DRX-300 NMR spectrometer and Varian Unity Inova 500 NMR spectrometer. Fluorescence imagings were obtained on a ZEISS Axio Scope A1 Fluorescence Microscope.

2.2. Synthesis of 5-(pyren-1-yl)-4,6-dipyrromethane (*1*):

To a stirred solution of 1-pyrenecarboxyaldehyde (1.25 g, 6.05 mmol) in pyrrole (21 mL, 0.3 mol) at 23 °C under N_2 atmosphere, trifluoroacetic acid (0.180 mL, 2.40 mmol) was added. After 30 min the reaction mixture was evaporated under reduced pressure. The residue was dissolved in dichloromethane (70 mL) and washed with a 1.0 M aqueous solution of NaOH (100 mL). The aqueous layer was extracted with dichloromethane (70 mL) and

* Corresponding author. Tel.: +886 3 5712121x56506; fax: +886 3 5723764.
E-mail addresses: spwu@mail.nctu.edu.tw, spwu@faculty.nctu.edu.tw (S.-P. Wu).

http://dx.doi.org/10.1016/j.snb.2014.07.049
0925-4005/

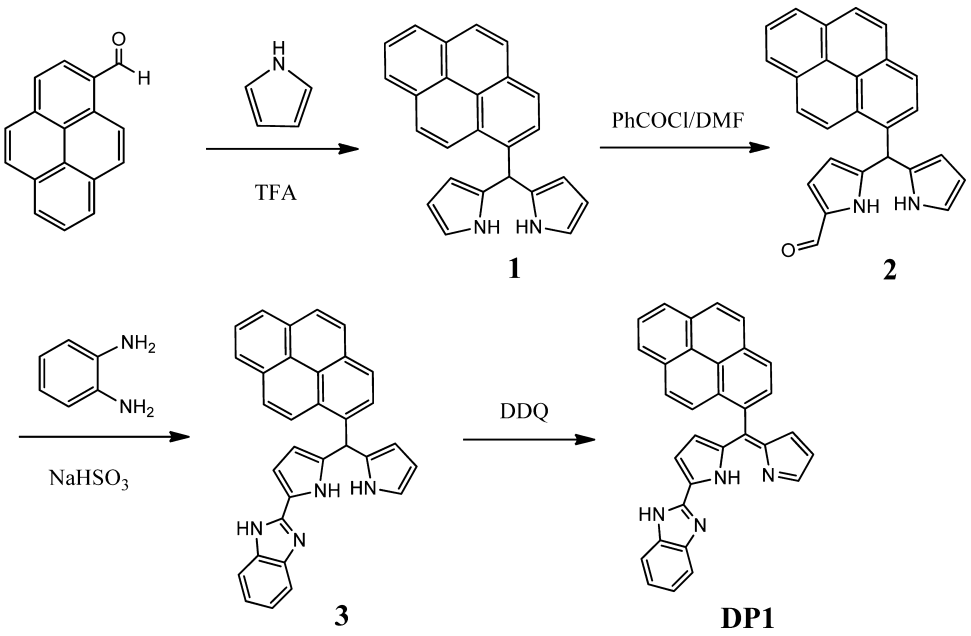

Scheme 1. Synthesis of DP1.

the combined organic layers were concentrated under reduced pressure. The residue was purified by silica gel chromatography (EtOAc/Hexane = 1/6) to give a compound **1** as a white solid (yield: 1.25 g, 60%). Melting point: 207–208 °C. ^{1}H NMR (300 MHz, DMSO-d_6): δ 10.74 (s, 2H), 8.45 (d, J = 9.3 Hz, 1H), 8.28 (d, J = 3.6 Hz, 1H), 8.26 (d, J = 3.3 Hz, 1H), 8.22 (d, J = 8.4 Hz, 2H), 8.16–8.13 (m, 2H), 8.07 (t, J = 7.6 Hz, 1H), 7.69 (d, J = 7.8 Hz, 1H), 6.66 (d, J = 1.2 Hz, 2H), 6.52 (s, 1H), 5.92 (d, J = 2.7 Hz, 2H), 5.62 (s, 2H). ^{13}C NMR (75 MHz, DMSO-d_6): δ 138.8, 134.1, 131.7, 131.1, 130.3, 128.7, 128.3, 127.6, 127.0, 126.9, 126.0, 125.7, 125.6, 124.9, 124.8, 124.3, 117.8, 107.9, 107.8, 40.6. MS (EI): m/z (%) = 346 (100), 278 (82), HRMS (EI): calcd. for $C_{25}H_{18}N_2$ (M^+) 346.1470; found: 346.1467.

2.3. Synthesis of 1-formyl-5-(pyren-1-yl)-4,6-dipyrromethane (**2**):

Benzoyl chloride (0.57 mL, 4.7 mmol) was added to a cooled DMF (2.0 mL, 26 mmol) and stirred 30 min. Compound **1** (1.0 g, 2.9 mmol) in DMF were added in the reaction mixture under N_2 atmosphere. The mixture was stirred at 0 °C for 2 h and then another 2 h at room temperature. The reaction mixture was quenched by addition of Na_2CO_3 (2.0 g) dissolved in 50% aquous EtOH (150 mL). The resulting solution was extracted with CH_2Cl_2 (100 mL × 2). The organic layer was dried over anhydrous $MgSO_4$ and the solvent was evaporated under reduced pressure. The crude product was purified by silica gel chromatography (EtOAc/Hexane = 1/6) to give a compound **2** as a gray solid (yield: 0.61 g, 57%). Melting point: 177–178 °C. ^{1}H NMR (300 MHz, CD_3CN): δ 9.39 (s, 1H), 8.39 (d, J = 9.6 Hz, 1H), 8.28 (d, J = 6.3 Hz, 1H), 8.25 (d, J = 5.1 Hz, 1H), 8.21 (d, J = 7.8 Hz, 1H), 8.17 (d, J = 9.3 Hz, 1H), 8.12 (d, J = 1 Hz, 2H), 8.06 (t, J = 7.5 Hz, 1H), 7.69 (d, J = 8.1 Hz, 1H), 6.96 (dd, J = 3.8 Hz, J = 2.4 Hz, 1H), 6.73 (dd, J = 4.2 Hz, J = 2.7 Hz, 1H), 6.67 (s, 1H), 6.07 (dd, J = 5.7 Hz, J = 2.7 Hz, 1H), 5.98 (dd, J = 3.6 Hz, J = 2.4 Hz, 1H), 5.79 (s, 1H). ^{13}C NMR (75 MHz, $CDCl_3$): δ 179.1, 143.2, 134.1, 132.7, 131.7, 131.3, 131.0, 130.9, 129.1, 128.8, 128.1, 127.8, 126.6, 126.6, 126.0, 125.8, 125.5, 125.4, 125.1, 122.9, 122.7, 118.3, 111.7, 109.2, 108.7, 41.2. MS (EI): m/z (%) = 374 (98), 278 (100), 201(41). HRMS (EI): calcd. for $C_{26}H_{18}N_2O$ (M^+): 374.1419; found: 374.1411.

2.4. Synthesis of 1-(2-benzoimidazoyl)-5-(pyren-1-yl)-4,6-dipyrromethane (**3**):

Compound **2** (150 mg, 0.4 mmol) and o-phenylenediamine (43 mg, 0.4 mmol) were thoroughly mixed in 5 ml of EtOH. Sodium hydrogen sulfite (62 mg, 0.6 mmol) was added to mixture and stirred at 80 °C for 8 h. The reaction mixture was cooled to room temperature, and concentrated at reduced pressure. The crude product was purified by column chromatography (ethyl acetate/hexane, 1:6) to give a red-orange solid. (Yield: 130 mg, 70%). Melting point 250–251 °C. ^{1}H NMR (300 MHz, DMSO-d_6): δ 12.4 (s, 1H), 11.9 (s, 1H), 10.8 (s, 1H), 8.55 (d, J = 9.6 Hz, 1H), 8.30 (d, J = 8.7 Hz, 1H), 8.28 (d, J = 6.0 Hz, 1H), 8.26 (d, J = 1.5 Hz, 1H), 8.23 (d, J = 9.0 Hz, 1H), 8.14–8.11 (m, 2H), 8.08 (t, J = 7.8 Hz, 1H), 7.77 (d, J = 8.1 Hz, 1H), 7.49 (d, J = 3.9 Hz, 1H), 7.40 (d, J = 3.9 Hz, 1H), 7.12 (d, J = 2.4 Hz, 1H), 7.09 (d, J = 2.4 Hz, 1H), 6.77 (t, J = 3.0 Hz, 1H), 6.71 (s, 1H) 6.70 (d, J = 1.8 Hz, 1H), 5.95 (dd, J = 5.4 Hz, J = 3.0 Hz, 1H), 5.81 (d, J = 2.4 Hz, 1H), 5.70 (s, 1H). ^{13}C NMR (75 MHz, $CDCl_3$): δ 146.8, 143.8, 138.1, 135.1, 134.0, 132.0, 131.6, 130.9, 130.7, 128.6, 127.9, 127.4, 126.3, 126.2, 125.5, 125.4, 125.3, 125.1, 124.9, 122.8, 121.8, 121.5, 121.2, 117.7, 117.3, 114.4, 110.5, 110.4, 108.6, 108.2, 40.7. MS(EI): m/z (%) = 462 (100), 395 (32), 278 (60), 261 (34). HRMS (EI): calcd. for $C_{32}H_{22}N_4$ (M^+): 462.1844; found: 462.1847.

2.5. Synthesis of ***DP1***

2,3-Dichloro-5,6-dicyano-1,4-benzoquinone (DDQ; 110 mg, 0.5 mmol) dissolved in THF (5 mL) was added to a solution of compound **3** (130 mg, 0.28 mmol) in THF (10 mL). After the solution was stirred for 30 min, the reaction mixture was evaporated under reduced pressure. The crude product was purified by column chromatography (ethyl acetate/hexane, 1:2) to give a red solid **DP1** (yield: 87 mg, 67%). Melting point: 239–240 °C, ^{1}H NMR (300 MHz, CD_3OD): δ 8.37 (d, J = 7.5 Hz, 1H), 8.33 (d, J = 7.5 Hz, 1H), 8.24 (d, J = 6.9 Hz, 3H), 8.10–8.06 (m, 2H), 8.05–8.01 (m, 2H), 7.71 (m, 2H), 7.59 (s, 1H), 7.39 (d, J = 2.7 Hz, 1H), 7.30 (d, J = 3.3 Hz, 1H), 7.19 (d, J = 4.5 Hz, 1H), 6.56 (d, J = 4.8 Hz, 1H), 6.30 (t, J = 2.7 Hz, 1H), 6.11 (d, J = 3.3 Hz, 1H). ^{13}C NMR (125 MHz, DMSO-d_6): δ 157.3, 149.3, 147.9, 144.2, 140.6, 135.2, 134.7, 133.4, 132.1, 131.5, 131.1, 130.9, 130.3, 129.8, 128.3, 128.1, 128.0, 127.4, 126.7, 126.6, 125.9, 125.0,

124.1, 124.0, 123.7, 123.6, 122.9, 122.1, 119.6, 115.8, 112.6, 111.8. MS (EI): m/z (%) = 460 (11), 335 (7.8), 277 (21). HRMS (EI): calcd. for $C_{32}H_{20}N_4$ (M^+) 460.1688; found: 460.1673.

2.6. Determination of the binding stoichiometry and the association constants for the binding of Zn(II) to **DP1**

The binding stoichiometry of **DP1**–Zn^{2+} complexes was determined from a Job plot. The fluorescence intensity at 560 nm was plotted against the molar fraction of **DP1** with a total concentration of the sensor and Zn^{2+} ion of 80.0 μM. The molar fraction at maximum emission intensity represents the binding stoichiometry of the **DP1**–Zn^{2+} complexes. The maximum emission intensity was reached at a molar fraction of 0.5. This result indicates that chemosensor **DP1** forms a 1:1 complex with Hg^{2+}. The apparent association constant (K_a) of **DP1**–Zn^{2+} complexes was determined by the Benesi–Hildebrand Equation (1) [29].

$$\frac{1}{(F - F_0)} = \frac{1}{\{K_a \times (F_{max} - F_0) \times [Zn^{2+}]\}} + \frac{1}{(F_{max} - F_0)} \quad (1)$$

where F is the fluorescence intensity at 560 nm at any given Zn^{2+} concentration, F_0 is the fluorescence intensity at 560 nm in the absence of Zn^{2+}, and F_{max} is the maxima fluorescence intensity at 560 nm in the presence of Zn^{2+} in solution. The association constant K_a was evaluated graphically by plotting $1/(F - F_0)$ against $1/[Zn^{2+}]$. Data were linearly fitted according to Equation (1) and the K_a value was obtained from the slope and intercept of the line.

2.7. Cell culture

The cell line RAW264.7 cells was provided by the Food Industry Research and Development Institute (Taiwan). RAW264.7 cells were grown in H-DMEM (Dulbecco's Modified Eagle's Medium, high glucose) supplemented with 10% FBS (Fetal Bovine Serum) in an atmosphere of 5% CO_2 at 37 °C.

2.8. Fluorescence imaging

The cells cultured in DMEM were treated with 10 mM solutions of Zn^{2+} (2 μL; final concentration: 20 μM) dissolved in sterilized PBS (pH 7.4) and incubated at 37 °C for 30 min. The treated cells were washed with PBS (2 mL × 3) to remove remaining metal ions. DMEM (2 mL) was added to the cell culture, which was then treated with a 10 mM solution of chemosensor **DP1** (2 μL; final concentration: 20 μM) dissolved in DMSO. The samples were incubated at 37 °C for 30 min. The culture medium was removed, and the treated cells were washed with PBS (2 mL × 3) before observation. Fluorescence imaging was performed with a ZEISS Axio Scope A1 Fluorescence Microscope. The cells were excited with a white light laser at 480 nm, and emission was collected at 535 ± 25 nm.

2.9. Computational methods

Quantum chemical calculations based on density functional theory (DFT) were carried out using a Gaussian 09 program. The ground-state structures of **DP1** and the **DP1**–Zn^{2+} complexes were computed using the density functional theory (DFT) method with the hybrid-generalized gradient approximation (HGGA) functional B3LYP. The 6-31G basis set was assigned to nonmetal elements (C, H, and N). For the **DP1**–Zn^{2+} complex, the LANL2DZ basis set was used for Zn^{2+}, whereas the 6-31G basis set was used for other atoms.

3. Result and discussion

3.1. Synthesis of **DP1**

The synthesis of chemosensor **DP1** is outlined in Scheme 1. Compound **1** was prepared by the condensation of 1-pyrenecarboxaldehyde and pyrrole. Compound **2** was obtained by the Vilsmeier–Haack reaction using benzoyl chloride and DMF to form mono formylated dipyrromethane. In the next step, condensation of *o*-phenylenediamine with compound **2** yielded

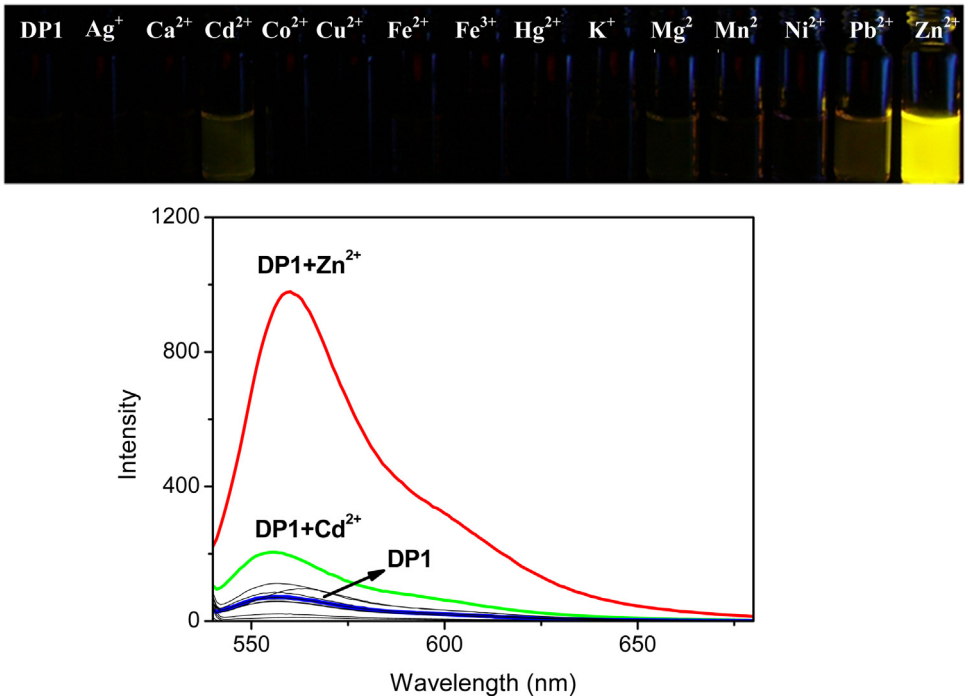

Fig. 1. (Top) Photographic images of **DP1** in the presence of various metal ions. (Bottom) Fluorescence change of **DP1** (20 μM) upon addition of various metal ions (20 μM) in methanol.

compound **3**. Further oxidation of compound **3** using DDQ gave the product **DP1**.

3.2. Metal ion sensing ability of *DP1*

The sensing ability of **DP1** was tested by mixing it with the metal ions Ca^{2+}, Cd^{2+}, Co^{2+}, Cu^{2+}, Fe^{2+}, Hg^{2+}, Mg^{2+}, Mn^{2+}, Ni^{2+}, and Zn^{2+}. Fig. 1 shows the effect of the metal ions on the appearance of **DP1** in solution. Zn^{2+} was the only ion that caused a yellow-green emission band at 560 nm. The other metal ions did not produce a great change in the emission spectra. During Zn^{2+} titration with chemosensor **DP1**, a new emission band centered at 560 nm was formed (Fig. 2). After the addition of more than one equivalent of Zn^{2+}, the emission intensity reached a maximum, with a quantum yield $\Phi = 0.103$, which is 20 times higher than that of **DP1**, at $\Phi = 0.005$. For the UV–vis absorption spectra, the absorbance at 477 nm decreased in intensity, and a new band centered at 540 nm appeared during Zn^{2+} titration with **DP1** (Fig. 2). The color change from yellow to purple clearly indicates the 63 nm blue shift. These observations suggest that Zn^{2+} is the only metal ion causing significant fluorescence enhancement, thereby permitting highly selective detection of Zn^{2+}.

To study the influence of other metal ions on Zn^{2+} binding with chemosensor **DP1**, we performed competitive experiments with other metal ions (20 μM) in the presence of Zn^{2+} (20 μM) (Fig. 3). The fluorescence enhancment caused by the mixture of Zn^{2+} with most other metal ions was similar to that caused by Zn^{2+} alone. A smaller fluorescence enhancement was observed when Zn^{2+} was mixed with Co^{2+} or Hg^{2+}. Fluorescence quenching was observed when Zn^{2+} was mixed with Cu^{2+}. This indicates that Co^{2+}, Hg^{2+}, and Cu^{2+} can compete with Zn^{2+} for binding with **DP1**. Most of the other metal ions do not interfere with the binding of **DP1** with Zn^{2+}.

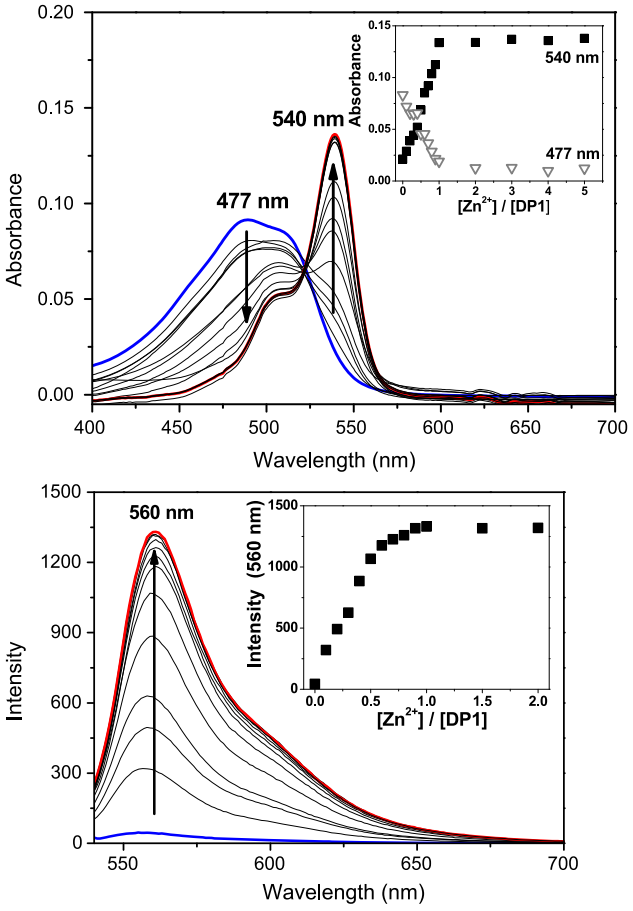

Fig. 2. Absorption (Top) and fluorescence (Bottom) changes of chemosensor **DP1** (20 μM) in the presence of various equivalents of Zn^{2+} in methanol. The excitation wavelength was 535 nm.

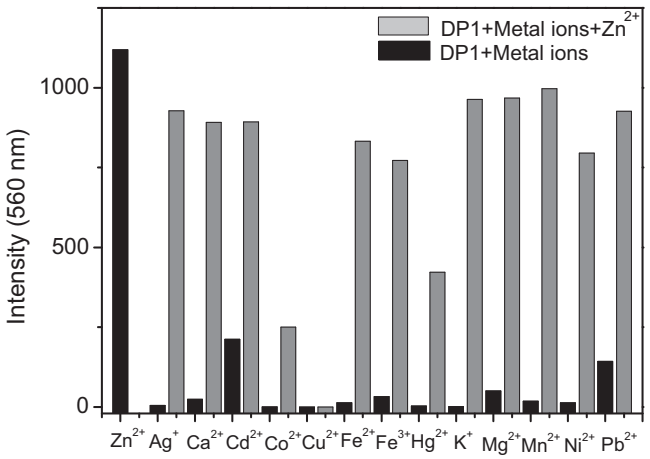

Fig. 3. Fluorescence response (560 nm) of chemosensor **DP1** (20 μM) to Zn^{2+} (20 μM) or 20 μM of other metal ions (the black bar portion) and to the mixture of other metal ions (20 μM) with 20 μM of Zn^{2+} (the gray bar portion).

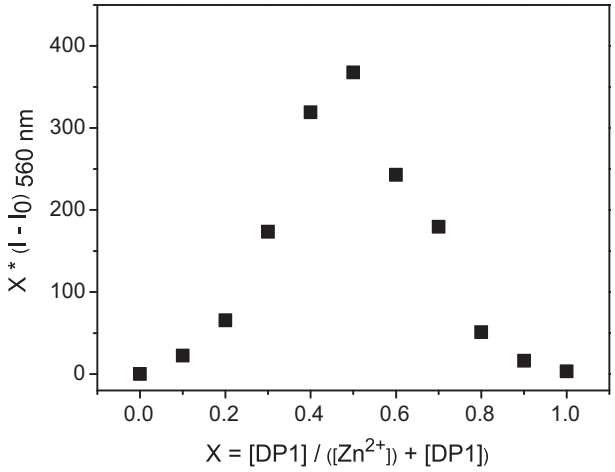

Fig. 4. Job plot of the **DP1**–Zn^{2+} complex in methanol. The total concentration of CBS and Zn^{2+} was 80 μM. The monitored wavelength was 560 nm.

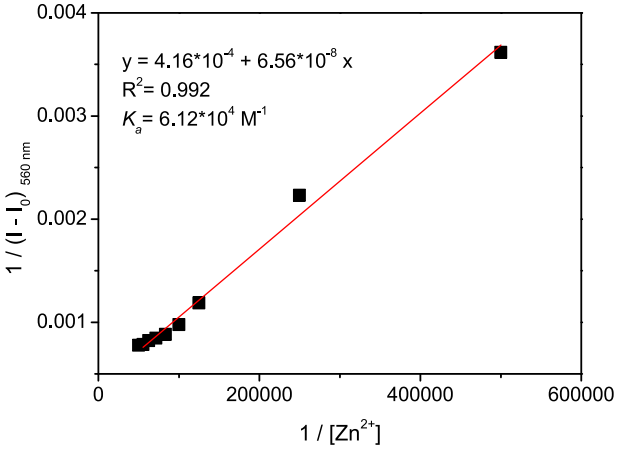

Fig. 5. Benesi–Hildebrand plot of DP1 with Zn^{2+} in methanol. The excitation wavelength was 535 nm and observed wavelength was 560 nm. The binding constant was $6.12 \times 10^4\ M^{-1}$ for Zn^{2+} binding in **DP1**.

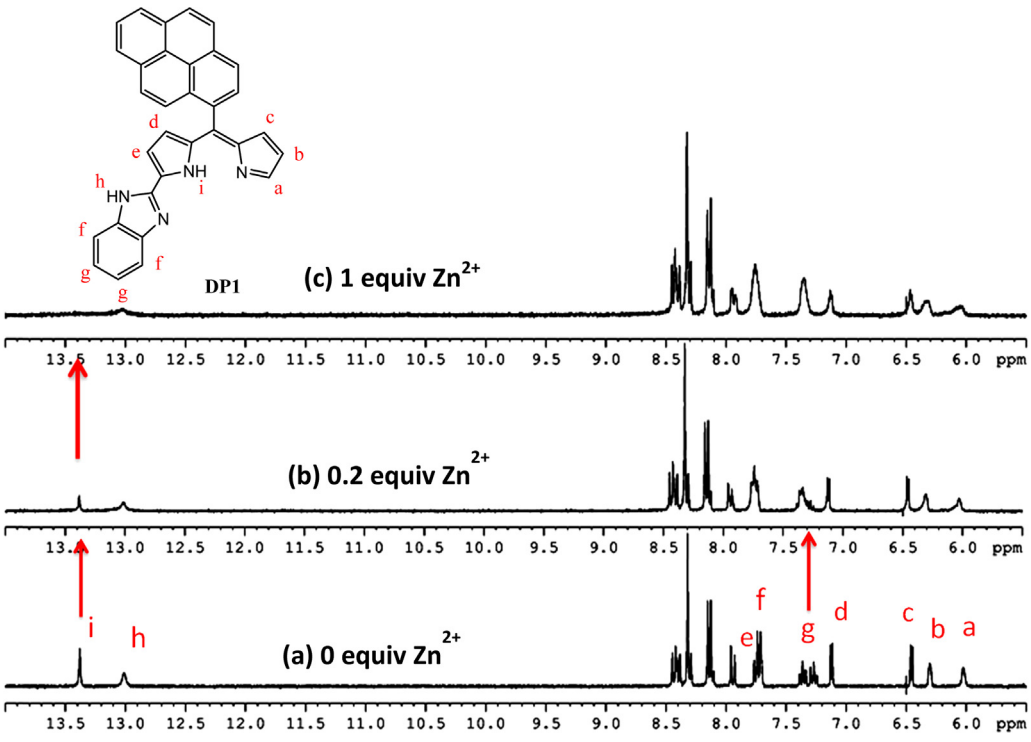

Fig. 6. ^{1}H NMR spectra of DP1 (5 mM) upon titration with (a) 0 equiv, (b) 0.2 equiv, (c) 1 equiv of Zn^{2+} in DMSO-d_6.

This indicates that the other metal ions do not interfere significantly with the binding of chemosensor **DP1** with Zn^{2+}.

In order to understand the binding stoichiometry of the **DP1**–Zn^{2+} complexes, Job plot experiments were carried out. In Fig. 4, the emission intensity at 560 nm is plotted against the molar fraction of **DP1** under a constant total concentration of **DP1** and Zn^{2+}. Maximum fluorescent enhancement occurred at the ratio 0.5. This result indicates a 1:1 ratio for **DP1**–Zn^{2+} complexes, in which one Zn^{2+} ion binds to one chemosensor **DP1**. In addition, the formation of 1:1 **DP1**–Zn^{2+} complexes was also confirmed using ESI-MS, in which the peak at m/z 541.1 indicates a 1:1 stoichiometry for **DP1**–Zn^{2+} complexes (see Fig. S9 in the supplementary data). The association constant K_a was evaluated graphically by plotting $1/(F - F_0)$ against $1/[Zn^{2+}]$ (Fig. 5). The data were linearly fit and the K_a value was obtained from the slope and intercept of the line. The association constant (K_a) of Zn^{2+} binding to chemosensor **DP1** was found to be 6.12×10^4 M^{-1}. The detection limit of chemosensor **DP1** as a fluorescent sensor for the detection of Zn^{2+} was determined from a plot of fluorescence intensity as a function of the concentration of Zn^{2+}. It was found that chemosensor **DP1** has a detection limit of 0.236 μM (see Fig. S10 in the supplementary data), which allows for the detection of Zn^{2+} in the micromolar concentration range.

To gain a clearer understanding of the structure of **DP1**–Zn^{2+} complexes, ^{1}H NMR spectroscopy (Fig. 6) was employed. In the ^{1}H NMR spectra of **DP1**, the proton signals at 13.4 and 13.0 ppm decreased upon addition of Zn^{2+}. This indicates that Zn^{2+} binding occurs mainly at the nitrogen atoms in pyrrole and benzoimidazole.

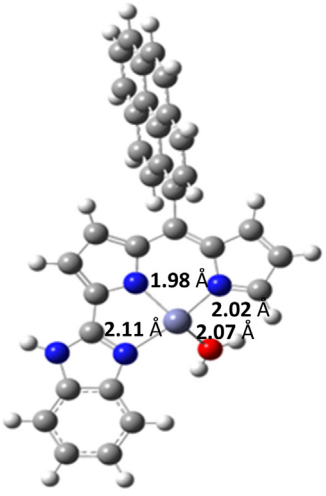

Fig. 7. DFT-optimized structures of **DP1**–Zn^{2+} complexes. Blue atom, N; red atom, O; gray atom, Zn^{2+}.(For interpretation of the references to color in this figure legend, the reader is referred to the web version of the article.)

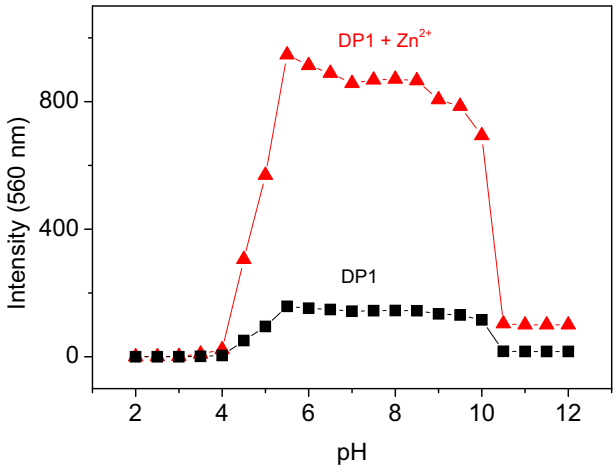

Fig. 8. Fluorescence response (560 nm) of free DP1 (20 μM) and after addition of Zn^{2+} (20 μM) in methanol–water (v/v = 9:1, 10 mM buffer, pH 2–4: sodium citrate/citratic acid; pH 4.5–6: MES; pH 6.5–8.5: Hepes; pH 9–12: Tris–HCl) solution as a function of different pH values. The excitation wavelength was 530 nm.

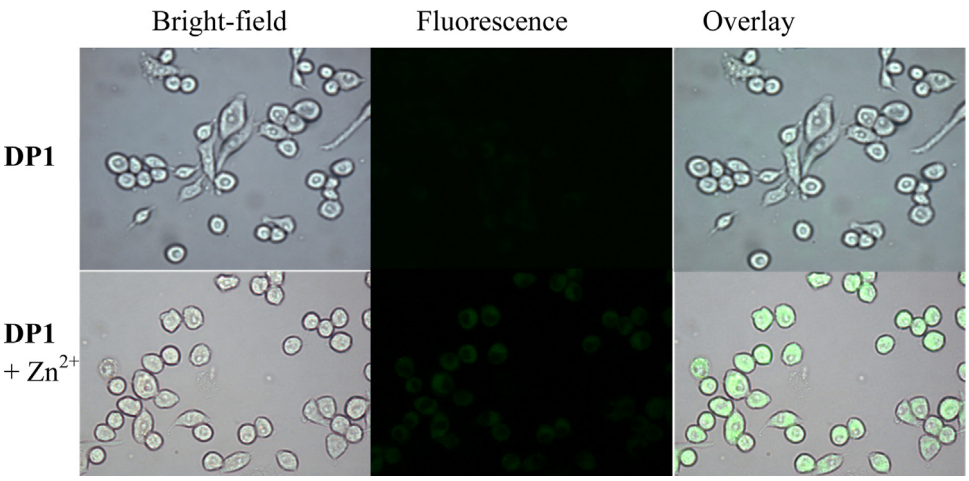

Fig. 9. Fluorescence images of RAW264.7 cells treated with **DP1** and Zn^{2+}. (Left) Bright field image; (middle) fluorescence image; (right) merged image.

These observations reveal that Zn^{2+} binding with **DP1** is through two nitrogens at pyrrole, and one nitrogen at benzoimidazole.

To elucidate the structures of the **DP1**–Zn^{2+} complexes, density functional theory (DFT) calculations were undertaken using the Gaussian 09 software package. The **DP1**–Zn^{2+} complexes were subjected to energy optimization using B3LYP/6-31G and B3LYP/LANL2DZ. The global minima structure for the **DP1**–Zn^{2+}complexes is shown in Fig. 7. The distances of Zn^{2+} from the three nitrogen atoms are about 2.0 and 2.1 Å.

We performed pH titration of chemosensor **1** to determine a suitable pH range for Zn^{2+} sensing. In Fig. 8, the emission intensities of metal-free chemosensor **1** at most pH values are low. After mixing chemosensor **1** with Zn^{2+}, the emission intensity at 560 nm suddenly increased in the pH range of 5.0–10.0. When the pH was lower than 5, the emission intensity at 560 nm decreased slightly, compared to that at pH 7.0. This is due to protonation on the nitrogen atom, preventing the formation of the Cu^{2+}–**1** complex.

3.3. *Living cell imaging*

The potential of **DP1** for imaging Zn^{2+} in living cells was then investigated. First, images of cells were obtained using a fluorescence microscope. When RAW264.7 cells were incubated with **DP1** (10 μM), no fluorescence was observed (Fig. 9a). After treatment with Zn^{2+}, bright green fluorescence was observed in the RAW264.7 cells (Fig. 9b). An overlay of the fluorescence and bright-field images shows that the fluorescence signals are localized in the intracellular area, indicating a subcellular distribution of Zn^{2+} and good cell-membrane permeability of **DP1**.

4. Conclusion

In conclusion, we developed a fluorescent chemosensor for Zn^{2+} detection. We observed significant fluorescence enhancement in the presence of Zn^{2+}. However, other metal ions, such as Ag^{+}, Ca^{2+}, Cd^{2+}, Co^{2+}, Cu^{2+}, Fe^{2+}, Fe^{3+}, K^{+}, Mg^{2+}, Mn^{2+}, Ni^{2+}, and Pb^{2+}, barely affected the fluorescence. In addition, this chemosensor **DP1** serves as an effective probe for Zn^{2+} detection in living cells.

Acknowledgments

We gratefully acknowledge the financial support of Ministry of Science and Technology (Taiwan, 101-2113-M-009-016-MY2) and National Chiao Tung University.

Appendix A. Supplementary data

Supplementary material related to this article can be found, in the online version, at http://dx.doi.org/10.1016/j.snb.2014.07.049.

References

[1] E.L. Que, D.W. Domaille, C.J. Chang, Metals in neurobiology: probing their chemistry and biology with molecular imaging, Chem. Rev. 108 (2008) 1517–1549.
[2] W. Maret, Y. Li, Coordination dynamics of Zinc in proteins, Chem. Rev. 109 (2009) 4682–4707.
[3] P.D. Zalewski, I.J. Forbes, W.H. Betts, Correlation of apoptosis with change in intracellular labile Zn(II) using Zinquin [(2-methyl-8-p-toluenesulphonamido-6-quinolyloxy)acetic acid], a new specific fluorescent probe for Zn(II), Biochem. J. 296 (1993) 403–408.
[4] K.H. Falchuk, The molecular basis for the role of zinc in developmental biology, Mol. Cell Biochem. 188 (1998) 41–48.
[5] A.I. Bush, W.H. Pettingell, G. Multhaup, M.D. Paradis, J. Vonsattel, J.F. Gusella, K. Beyreuther, C.L. Masters, R.E. Tanzi, Rapid induction of Alzheimer Aβ amyloid formation by Zinc, Science 265 (1994) 1464–1467.
[6] P.O. Tsvetkov, I.A. Popov, E.N. Nikolaev, A.I. Archakov, A.A. Makarov, S.A. Kozin, Isomerization of the Asp7 residue results in Zinc-induced oligomerization of Alzheimer's disease amyloid β(1–16) peptide, Chem. BioChem. 9 (2008) 1564–1567.
[7] G. Wei, C.J. Hough, Y. Li, J.M. Sarvey, Characterization of extracellular accumulation of Zn^{2+} during ischemia and reperfusion of hippocampus slices in rat, Neuroscience 125 (2004) 867–877.
[8] J. Kapur, R.L. Macdonald, Rapid seizure-induced reduction of benzodiazepine and Zn^{2+} sensitivity of hippocampal dentate granule cell GABAA receptors, J. Neurosci. 17 (1997) 7532–7540.
[9] C.R.T. Tarley, F.N. Andrade, F.M. de Oliveira, M.Z. Corazza, L.F.M. de Azevedo, M.G. Segatelli, Synthesis and application of imprinted polyvinylimidazole - silica hybrid copolymer for Pb^{2+} determination by flow-injection thermospray flame furnace atomic absorption spectrometry, Anal. Chim. Acta 703 (2011) 145–151.
[10] H. Karami, M.F. Mousavi, Y. Yamini, M. Shamsipur, On-line preconcentration and simultaneous determination of heavy metal ions by inductively coupled plasma-atomic emission spectrometry, Anal. Chim. Acta 509 (2004) 89–94.
[11] L. Zhao, S. Zhong, K. Fang, Z. Qian, J. Chen, Determination of cadmium(II), cobalt(II), nickel(II), lead(II), zinc(II), and copper(II) in water samples using dual-cloud point extraction and inductively coupled plasma emission spectrometry, J. Hazard. Mater. 239–240 (2012) 206–212.
[12] F. Tormaa, M. Kadar, K. Toth, E. Tatar, Nafion®/2,2.-bipyridyl-modified bismuth film electrode for anodic stripping voltammetry, Anal. Chim. Acta 619 (2008) 173–182.
[13] J. Wu, W. Liu, X. Zhuang, F. Wang, P. Wang, S. Tao, X. Zhang, S. Wu, S. Lee, Fluorescence turn on of coumarin derivatives by metal cations: a new signaling mechanism based on C=N isomerization, Org. Lett. 9 (2007) 33–36.
[14] H.S. Jung, K.C. Ko, J.H. Lee, S.H. Kim, S. Bhuniya, J.Y. Lee, Y. Kim, S.J. Kim, J.S. Kim, Rationally designed fluorescence turn-on sensors: a new design strategy based on orbital control, Inorg. Chem. 49 (2010) 8552–8557.
[15] Z. Li, M. Yu, L. Zhang, M. Yu, J. Liu, L. Wei, H. Zhang, A "switching on" fluorescent chemodosimeter of selectivity to Zn^{2+} and its application to MCF-7 cells, Chem. Commun. 46 (2010) 7169–7171.
[16] Z. Xu, K. Baek, H.N. Kim, J. Cui, X. Qian, D.R. Spring, I. Shin, J. Yoon, Zn^{2+}-triggered amide tautomerization produces a highly Zn^{2+}-selective, cell-permeable, and ratiometric fluorescent sensor, J. Am. Chem. Soc. 132 (2010) 601–610.

[17] G. Sivaraman, T. Anand, D. Chellappa, Turn-on fluorescent chemosensor for Zn(II) via ring opening of rhodamine spirolactam and their live cell imaging, Analyst 137 (2012) 5881–5884.
[18] A. Ganguly, B.K. Paul, S. Ghosh, S. Kar, N. Guchhait, Selective fluorescence sensing of Cu(II) and Zn(II) using a new Schiff base-derived model compound: naked eye detection and spectral deciphering of the mechanism of sensory action, Analyst 138 (2013) 6532–6541.
[19] W. Lin, D. Buccella, S.J. Lippard, Visualization of peroxynitrite-induced changes of labile Zn^{2+} in the endoplasmic reticulum with benzoresorufin-based fluorescent probes, J. Am. Chem. Soc. 135 (2013) 13512–13520.
[20] H. Woo, S. Cho, Y. Han, W. Chae, D. Ahn, Y. You, W. Nam, Synthetic control over photoinduced electron transfer in phosphorescence Zinc sensors, J. Am. Chem. Soc. 135 (2013) 4771–4787.
[21] S. Cui, G. Liu, S. Pu, B. Chen, A highly selective fluorescent probe for Zn^{2+} based on a new photochromic diarylethene with a di-2-picolylamine unit, Dyes Pigm. 99 (2013) 950–956.
[22] T. Zhang, F. Wang, M. Li, J. Liu, J. Miao, B. Zhao, A simple pyrazoline-based fluorescent probe for Zn^{2+} in aqueous solution and imaging in living neuron cells, Sens. Actuators B 186 (2013) 755–760.
[23] Y. Ma, F. Wang, S. Kambam, X. Chen, A quinoline-based fluorescent chemosensor for distinguishingcadmium from zinc ions using cysteine as an auxiliary reagent, Sens. Actuators B 188 (2013) 1116–1122.
[24] J. Ma, R. Sheng, J. Wu, W. Liu, H. Zhang, A new coumarin-derived fluorescent sensor with red-emission for Zn^{2+} in aqueous solution, Sens. Actuators B 197 (2014) 364–369.
[25] Y.J. Lee, C. Lim, H. Suh, E.J. Song, C. Kim, A multifunctional sensor: chromogenic sensing for Mn^{2+} and fluorescent sensing for Zn^{2+} and Al^{3+}, Sens. Actuators B 201 (2014) 535–544.
[26] S.S. Mati, S. Chall, S. Konar, S. Rakshit, S.C. Bhattacharya, Pyrimidine-based fluorescent zinc sensor: photo-physicalcharacteristics, quantum chemical interpretation and applicationin real samples, Sens. Actuators B 201 (2014) 204–212.
[27] M. Iniya, D. Jeyanthi, K. Krishnaveni, A. Mahesh, D. Chellappa, Triazole based ratiometric fluorescent probe for Zn^{2+} and its application in bioimaging, Spectrochim. Acta Part A 120 (2014) 40–46.
[28] G. Sivaraman, T. Anand, D. Chellappa, Pyrene based selective–ratiometric fluorescent sensing of zinc and pyrophosphate ions, Anal. Methods 6 (2014) 2343–2348.
[29] H.A. Benesi, J.H. Hildebrand, A spectrophotometric investigation of the interaction of iodine with aromatic hydrocarbons, J. Am. Chem. Soc. 71 (1949) 2703–2707.

Biographies

Hao-Ming Liu had MS in 2012, Department of Applied Chemistry at National Chiao Tung University.

Parthiban Venkatesan is studying for Ph.D. in the Department of Applied Chemistry at National Chiao Tung University.

Dr. Shu-Pao Wu had Ph.D. in 2004, Department of Chemistry, The Ohio State University, USA. Currently, he is working as an Associate Professor in Department of Applied Chemistry National Chiao Tung University, Taiwan, Republic of China. Current interests: metal ion chemosensors and AlkB.